Int. J. Electron. Commun. (AEÜ) ▮ (▮▮▮▮) ▮▮▮–▮▮▮

Contents lists available at ScienceDirect

Int. J. Electron. Commun. (AEÜ)

journal homepage: www.elsevier.de/aeue

Two novel very small monopole antennas having frequency band notch function using DGS for UWB application

Saber Soltani [a,b,*], Mohammadnaghi Azarmanesh [a], Parisa Lotfi [a], Gholamreza Dadashzadeh [c]

[a] Microelectronics Research Laboratory, Urmia University, Urmia, Iran
[b] Young Researchers Club, Islamic Azad University, Urmia, Iran
[c] Department of the Electrical Engineering, Shahed University, Tehran, Iran

ARTICLE INFO

Article history:
Received 7 September 2009
Accepted 1 January 2010

Keywords:
Asymmetric coplanar strip (ACS) feed
Coplanar wave-guide (CPW) feed
Frequency band notch
Monopole antennas

ABSTRACT

In this article, we describe two novel types of coplanar wave-guide (CPW) fed monopole and an asymmetric coplanar strip (ACS) fed half monopole UWB antennas to cover the ultra-wideband frequency operation. The proposed antennas consist of a hexagonal shaped patch with small volume ($18.4 \times 21.5 \times 1\,mm^3$) and ($11.4 \times 21.5 \times 1\,mm^3$), respectively. The band-rejection operation achieve at the WLAN (5.15–5.85 GHz) band by adding defected ground structure (DGS) or slit in the ground plane. The antennas are fabricated on FR4 substrate with a relative dielectric constant of 4.4 and thickness of 1 mm which are fed by a 50 Ω line. The antennas are investigated numerically and experimentally for their impedance matching properties, frequency notched characteristics, and radiation performances. The measured frequency response shows an impedance bandwidth of 13 GHz or 130% over 3–16 GHz for VSWR < 2.

1. Introduction

In recent years, more interest has been put into wireless personal area network (WPAN) technology. The future WPAN aims to provide reliable wireless connections between computers, portable devices and consumer electronics within a short range. Furthermore, fast data storage and exchange between these devices will also be accomplished. This requires a data rate which is much higher than what can be achieved through currently existing wireless technologies. Since the protocol of the ultra-wideband (UWB) wireless communications released by the Federal Communications Commission (FCC) in 2002 [1] that covers the frequency range from 3.1 to 10.6 GHz, the design of UWB antennas has become a particularly challenging theme. In ultra-wideband (UWB) communications, the antennas are small size, high data transmission rates [2], large bandwidth enables short-range, low power consumption, simple hardware configuration, omni-directional radiation pattern (small directivity), low group delay, constant gain, and a linear phase response. These antennas could be applied in radar, location tracing, sensor networks, and data transmissions. For UWB antennas that are electrically small and the radiation pattern is almost constant with frequency. Due to their attractive features, planar monopole antennas have been good candidate for UWB communication systems. Several planar UWB antennas, which have the potential to meet such requirements, were reported in [3–6]. The UWB communication systems use the 3.1–10.6 GHz frequency band, which includes HIPERLAN/2 bands (5.15–5.35 and 5.470–5.725 GHz) and the IEEE 802.11a bands (5.15–5.35 and 5.725–5.825 GHz). Therefore, UWB communication systems may generate interference with IEEE802.11a and HIPERLAN/2 bands. To avoid the interference between the UWB and WLAN systems, a band-notch filter in UWB system is necessary. Anyway, the use of a filter will increase the complexity of the UWB system. To overcome electromagnetic interference between UWB and WLAN system, various UWB antennas by different researchers in order to design compact antennas with the desired features have been reported. Generally, there are few simple ways for monopole planar antennas to achieve a band-notched characteristic. The conventional methods to achieve a notched band are cutting proper slot (such as a U-shaped slot [7,8], a ⋂- shaped slot [9], and a bent slot or C-shaped slot [10]) or embedding a quarter-wavelength tuning stub within a large slot on the patch [11]. Another way is to put parasitic elements near the printed monopole, playing a role as filters to reject the limited band [12]. Folded strip patch [13],C-shaped attachment element in patch [14], are playing a role as filter to reject a sub-band. These methods can achieve a good band-notched characteristic and cause little complexity in the design procedure of the UWB antennas. Based on the background of the research above, we

* Corresponding author at: Microelectronics Research Laboratory, Urmia University, Urmia, Iran. Tel./fax: +98 441 3452807.
E-mail addresses: st_s.soltani@mail.urmia.ac.ir (S. Soltani), m.azarmanesh@urmia.ac.ir (M. Azarmanesh), ps.lotfi@gmail.com (P. Lotfi), gdadashzadeh@shahed.ac.ir (G. Dadashzadeh).

1434-8411/$ - see front matter © 2010 Elsevier GmbH. All rights reserved.
doi:10.1016/j.aeue.2010.01.013

propose two CPW-fed monopole and asymmetric coplanar strip ACS-fed half monopole UWB antennas with band-notch characteristics fabricated on low cost (1 mm) FR4 substrate. The HFSS v10 (method of finite-element by Ansoft) was used to predict the performance of antennas [15]. The configuration and design method of UWB CPW-fed antenna geometry and details of the antenna design are introduced in Section 2. The simulated and measured results of CPW-fed antenna are shown in Section 3. Section 4 presents ACS-fed antenna geometry with details of the antenna design and comparison measurement results of both antennas. The conclusions are made in Section 5.

2. UWB CPW-fed monopole antenna design

2.1. Antenna configuration

Fig. 1 shows the geometry of the proposed CPW-fed antenna. The 50 Ω CPW-fed monopole antenna is printed on standard FR4 epoxy substrate with thickness of h = 1 mm and relative permittivity of $\varepsilon_r = 4.4$ and loss tangent of (around 0.02). The use of low-cost FR4 as substrate introduces some additional complexity on the antenna design. This additional complexity is due to the inaccuracy of the FR4 relative permittivity and its high loss tangent. Variations in the FR4 electrical permittivity can shift the operating frequency. A CPW transmission line with a signal strip width W_f = 2.4 mm and gap width between the ground plane and signal strip g = 0.3 mm and the two equal finite coplanar rectangular ground plane ($W_g \times L_g$) is used to feed the monopole antenna. The feed of the CPW-fed antenna is designed using standard design equations [16]. The proposed monopole antenna consists of two parts: hexagonal shape patch, with has the heights (L_f, L_3, L_4) and widths (W_3, W_4) provide UWB performance and two symmetric slits in the ground plane with height (L_1, L_2) and widths (W_1, W_2) prevent interference with the WLAN band around 5.5 GHz. For compact UWB antenna the ground size is critical for the overall antenna performance. Nevertheless, the slit width of g_{slit} is practically constrained to a lower limit of 0.2 mm due to the manufacturing tolerance. It is known that the equivalent L–C components of defects give rise to form a band-rejection characteristic [17].

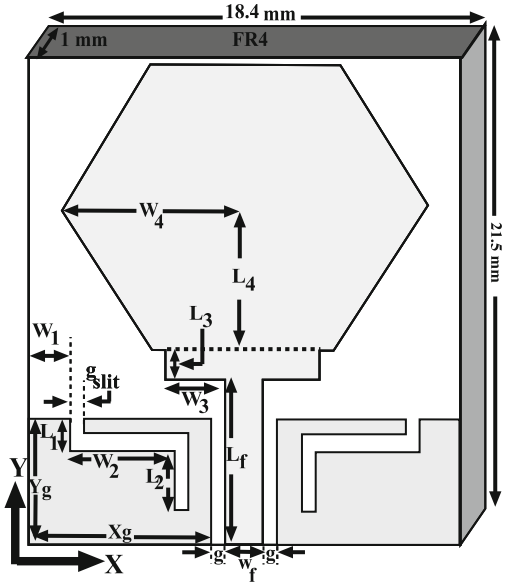

Fig. 1. Geometry of the proposed monopole antenna (unit: mm).

Table 1
Dimensions of CPW-fed monopole antenna (units in mm).

W_f	g	L_f	L_g	W_1	L_1
2.4	0.3	7.7	4.35	2.8	0.7
W_2	L_2	W_3	L_3	W_4	L_4
4.2	3.15	2.4	1.9	8.2	7.1

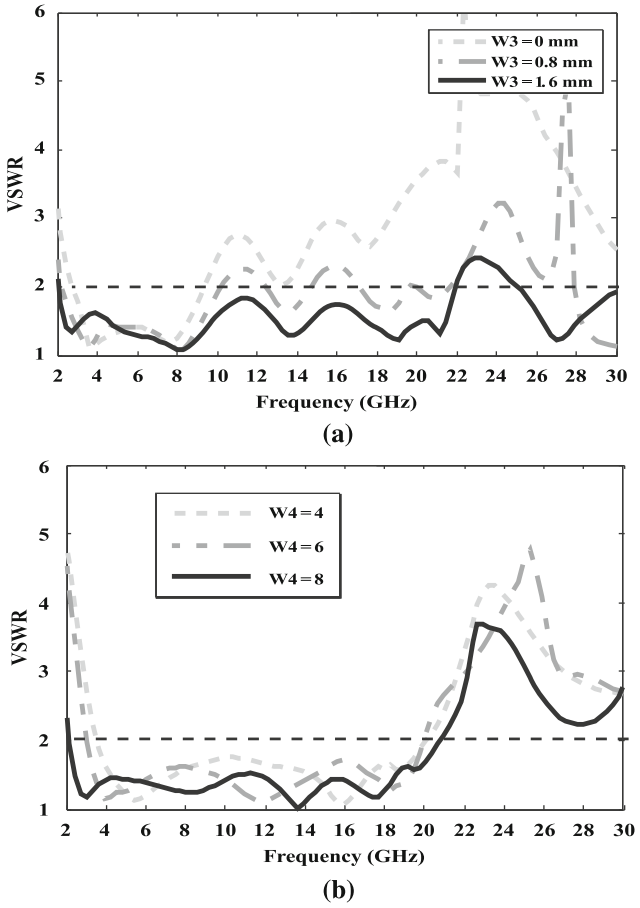

Fig. 2. Relations between the VSWR and dimensions of the proposed antenna (in millimeter): (a) variations of W_3 with fixed other optimized dimensions without DGS and (b) variations of W_4 with fixed other optimized dimensions without DGS.

The dimensions of antenna using SA (simulation analysis) or parametric analysis and designer's experience are listed in Table 1 (units in mm).

2.2. Effects of the geometrical parameters on antenna performance

Every geometrical parameter has different effects on the performance of the proposed antenna. In the following text, seven parts of the proposed CPW-fed monopole antenna that will be described and discussed, respectively: (1) W_3: rectangular width of patch ; (2) W_4: hexagonal width of patch; (3) W_1: DGS slits distance (width) from substrate edge; (4) L_1: first step of DGS slits length; (5) W_2: second step of DGS slits width; (6) L_2: second step of DGS slits length; and (7) g_{slit}: slit width.

2.2.1. The effect of rectangular width of patch (W_3)

Fig. 2(a) gives the simulated VSWR of the antenna as a function of frequency for different values of W_3 with fixed other optimized parameters of the patch and without DGS. From Fig. 2(a), one can find that the change of W_3 has significant effects on the bandwidth of the proposed antenna. Therefore, that region plays an important

Please cite this article as: Soltani S, et al. Two novel very small monopole antennas having frequency band notch function using DGS for UWB application. Int J Electron Commun (AEU) (2010), doi:10.1016/j.aeue.2010.01.013

role in impedance matching. From the simulation results in Fig. 2(a), it is observed that the impedance bandwidth at the upper operating frequency increases as the length W_3 increases. Also it is seen that the additional resonances occur at 14 and 20 GHz but lower operating frequency remains almost unchanged. This is due to the capacitive and inductive effects caused by the electromagnetic coupling effects between the patch and ground planes [18].

2.2.2. The effect of the hexagonal width of patch (W_4)

The dimensions of the top part of patch have a most pronounced effect at the lower operating frequency. The simulated VSWR curves with different values of W_4 with fixed other optimized parameters of the patch and without DGS are plotted in Fig. 2(b). From the simulation results in Fig. 2(b), it is seen that the impedance bandwidth performance at the lower band edge increases as the W_4 increases. Fortunately it can be seen that increasing the parameter of W_4 also improves the performance at the upper band edge.

2.2.3. The effect of the DGS slits distance (width) from substrate edge (W_1)

Fig. 3(a) shows simulated VSWR characteristics with the optimum dimension for parameters and for different values of W_1. As the DGS slit's distance (width) from substrate edge (W_1) increases from 1 to 3 mm, the center frequency of notched band is varied from 5.99 to 5.43 GHz. It can be seen that the VSWR of the center frequency of the notch is varied from 3.2 to 6.8. From this result, one can conclude that the VSWR of the center frequency of the notch and filtering frequency is controllable by changing the width of W_1.

2.2.4. The effect of first step of DGS slits length (L_1)

The effect of the length of the DGS on antenna performance is studied by varying L_1, as shown in Fig. 3(b) (other dimension is fixed). As the L_1 increases from 0.5 to 0.9 mm, the center frequency of notched band is varied from 5.95 to 5.25 GHz. It can be seen that the VSWR of the center frequency of the notch and bandwidth of the notch remains almost fixed.

2.2.5. The effect of second step of DGS slits width (W_2)

Fig. 3(c) indicates the simulated VSWR results for proposed antenna in terms of W_2. For W_2 =1.8, 3 and 3.8 mm with other fixed dimensions, the notch frequencies decrease from 9 to 6.26 GHz. It can be seen that tuning the width W_2 has significant effects on shifting the notch frequency. In this case this variation provides a very regular tuning effect.

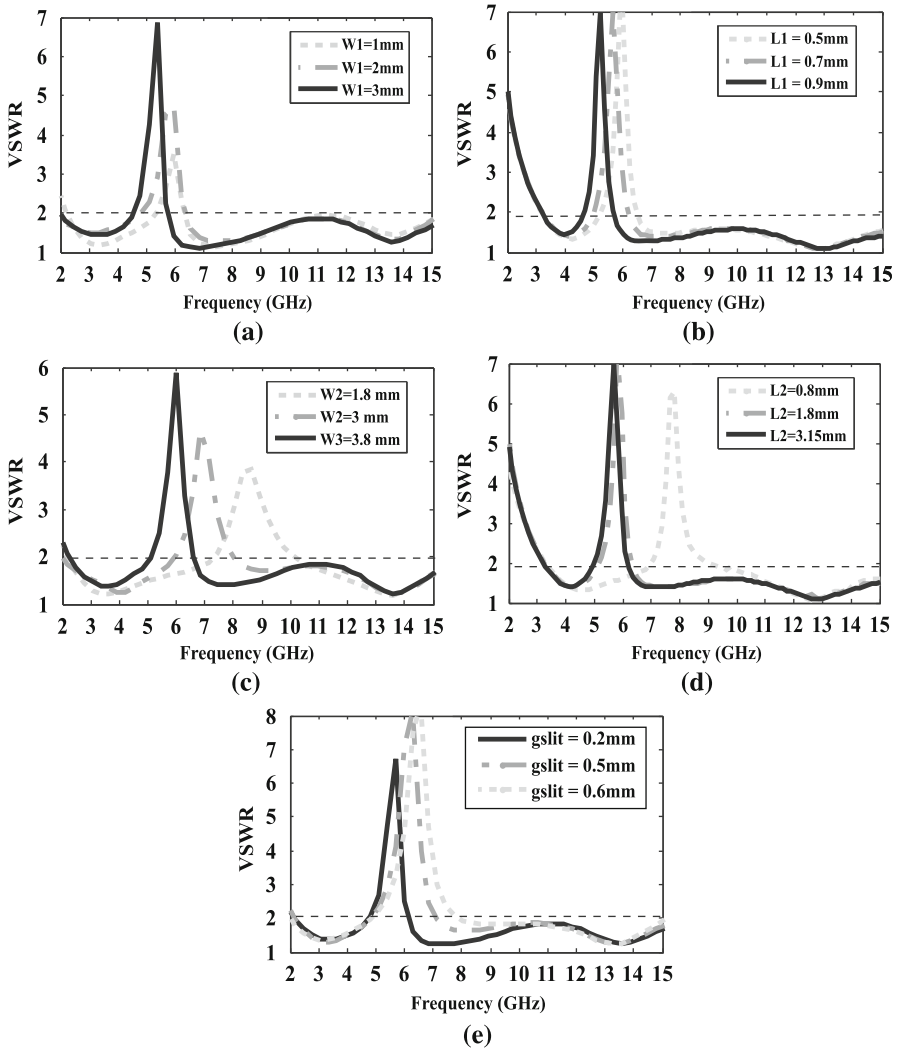

Fig. 3. Relations between the VSWR and the dimensions of the proposed antenna (in millimeter): (a) variations of W_1 with fixed other optimized dimensions; (b) variations of L_1 with fixed other optimized dimensions; (c) variations of W_2 with fixed other optimized dimensions; (d) variations of L_2 with fixed other optimized dimensions; and (e) variations of g_{slit} with fixed other optimized dimensions.

Please cite this article as: Soltani S, et al. Two novel very small monopole antennas having frequency band notch function using DGS for UWB application. Int J Electron Commun (AEU) (2010), doi:10.1016/j.aeue.2010.01.013

Table 2
Center frequency of rejection band.

W_2	L_2	L_1	g_{slit}	L Fig3	L Eq. (1)	f Fig3	f Eq. (1)	$f_{Fig.\ 3} - f_{Eq.\ (1)}$
4.2	3.15	0.3	0.2	5.74	5.92	6.23	6.07	0.16
4.2	3.15	0.5	0.2	6.01	6.13	5.95	5.87	0.08
4.2	3.15	0.7	0.2	6.29	6.53	5.68	5.5	0.18
4.2	3.15	0.9	0.2	6.81	6.92	5.25	5.18	0.07
4.2	3.15	1.1	0.2	6.99	7.16	5.11	5.01	0.1
4.2	2.8	0.7	0.2	6.11	6.1	5.85	5.91	0.06
4.2	3.15	0.7	0.2	6.33	6.53	5.65	5.51	0.14
3	3.15	0.7	0.2	5.12	5.35	7	6.71	0.29
3.6	3.15	0.7	0.2	5.55	5.65	6.44	6.35	0.09
3.8	3.15	0.7	0.2	5.71	5.85	6.26	6.13	0.13
4	3.15	0.7	0.2	5.96	6.14	6	5.85	0.15
4.2	3.15	0.7	0.2	6.33	6.53	5.65	5.5	0.15
4.4	3.15	0.7	0.2	6.99	7.04	5.11	5.1	0.01
4.2	3.15	0.7	0.2	6.5	6.53	5.5	5.5	0
4.2	3.15	0.7	0.5	5.5	5.52	6.51	6.5	0.01
4.2	3.15	0.7	0.8	5.26	5.27	6.8	6.81	0.01

2.2.6. The effect of the second step of DGS slits length (L_2)

The simulated VSWR curve with different values of L_2 is plotted in Fig. 3(d). As the L_2 increases from 0.8 to 3.15 mm with other fixed dimensions, the filtering frequency is varied from 7.7 to 5.65 GHz. It can be seen that it is irregular.

2.2.7. The effect of slit width (g_{slit})

Fig. 3(e) shows that the DGS slits width (g_{slit}) increases from 0.2 to 0.6 mm; the filter bandwidth is varied from 1 to 2.5 GHz. It can be seen that tuning the width g_{slit} can shift the upper notched band edge, while the lower notched band edge remains almost fixed. Additionally, the numbers of turns of defected-slit and number of DGS elements are factors in determining the band-rejection characteristics. The relation between central notched frequencies and L_{notch} can be expressed approximately based on results of Figs. 3(a)–(e) as follows:

$$L_{notch} = (4.2g_{slit}^2 - 6.3g_{slit} + 41.2) + (0.43W_2^3 - 3.86W_2^2 + 11.9W_2 - 392.43) + (0.1L_2^2 + 0.7L_2 - 312.8) + (-3.61L_1^3 + 7.65L_1^2 - 3.3L_1 + 694.5) - 40 = \frac{\lambda_d}{4} = \frac{35.5}{f_{notch}} \quad (1)$$

where λ_d is dielectric wave length, f_{notch} is center of the undesired band and c is the speed of light in free space and ε_r is the dielectric constant. Table 2 shows comparison data between central notched frequencies in Figs. 3(a)–(e) and (1).

3. Results and discussion

3.1. Impedance bandwidth

The implemented dimensions of geometry parameters of CPW fed monopole antenna is chosen to achieve the optimum performance as predicted from parametric analysis that was described in Section 2. Fig. 4 shows the measured versus simulated frequency response of the voltage standing wave ratio (VSWR) for the proposed antenna. The VSWR was measured using an Agilent 8722ES network analyzer. The measured impedance bandwidth, defined by 2 VSWR, is about 13 GHz starting from 3 to 16 GHz including the notched bands of the IEEE 802.11a in the US and the HIPERLAN/2 in Europe, the notched bandwidth of a measured value is 1 GHz from 5 to 6 GHz. Comparison between simulated results and the measured results show reasonable agreement at the lower frequency. However, the measured result displays slightly difference at operating frequency. This may be due to small parametric differences present in the FR4 substrate between the practical embodiment and simulated models. It is also possible that the dielectric constant and dissipation factor has some variation with frequencies. Errors in the measurement also can be expected owing to the feed cable placed in the near field of the antenna. During measurements, care was taken to place a sheet of absorber material underneath the connector of antenna. Thus, almost no surface waves are excited in the measurement process from connector.

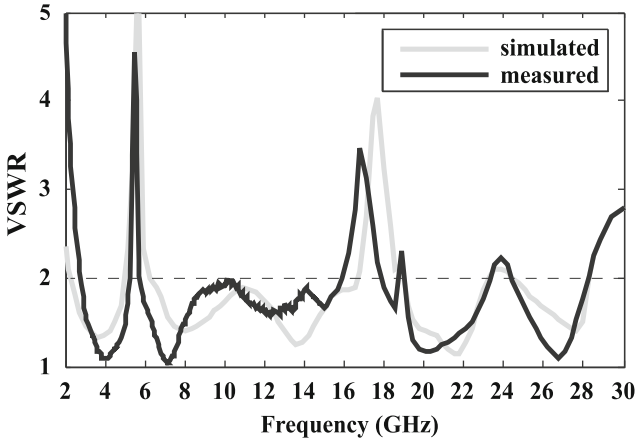

Fig. 4. Measured and simulated VSWR CPW-fed antenna.

3.2. Radiation pattern and gain results

The normalized simulated and measured E- and H-planes radiation patterns and simulated current distribution at 4, 7, and 10 GHz are shown in Figs. 5(a)–(c), respectively. The gain and radiation patterns were measured using the ETS 3115 system. The co and cross-polarized components of the field are different in the x–z (H-plane) and y–z (E-plane) plane. In the H-plane, the co-polarized component is E_φ, the cross-polarized component is E_θ. It is contrary in the E-plane. In the H-plane, the radiation pattern is omni-directional at lower frequency and is nearly omni-directional at higher frequency. In the E-plane, the radiation pattern is nearly bidirectional as a traditional monopole antenna. Fig. 6 shows the proposed antenna with band notch function peak gain from 3 to 11 GHz. The simulated and measured peak gain with frequency among x–z, y–z, and x–y planes is selected for the proposed antenna. It reveals that the antenna gain ranges from 1 to 4.5 dBi within 3–10.6 GHz frequency band; Of course, except for the notched band (5–6 GHz) where the gain decreases even to −9 dBi. It can be seen that for the frequency notch band the peak gain is negative, which is expected based on the VSWR results.

4. Miniaturization simulation and measurement results of band-notch UWB monopole antenna

4.1. Half monopole antenna design

Fig. 7 shows the miniaturized half hexagonal patch layout. It is fed by an asymmetric coplanar strip. The ACS exhibits very advantages of the CPW-fed antenna, such as: more compactness, a single lateral ground plane, wider impedance matching [19–21]. In the monopole antenna take into feeding structure and reducing the size, standing wave convert to traveling wave or hybrid wave (standing wave + traveling wave) that increase bandwidth at high frequency [22]. The ACS fed antenna, compared to CPW fed antenna also exhibits similar radiation patterns at E-plane but the

Please cite this article as: Soltani S, et al. Two novel very small monopole antennas having frequency band notch function using DGS for UWB application. Int J Electron Commun (AEU) (2010), doi:10.1016/j.aeue.2010.01.013

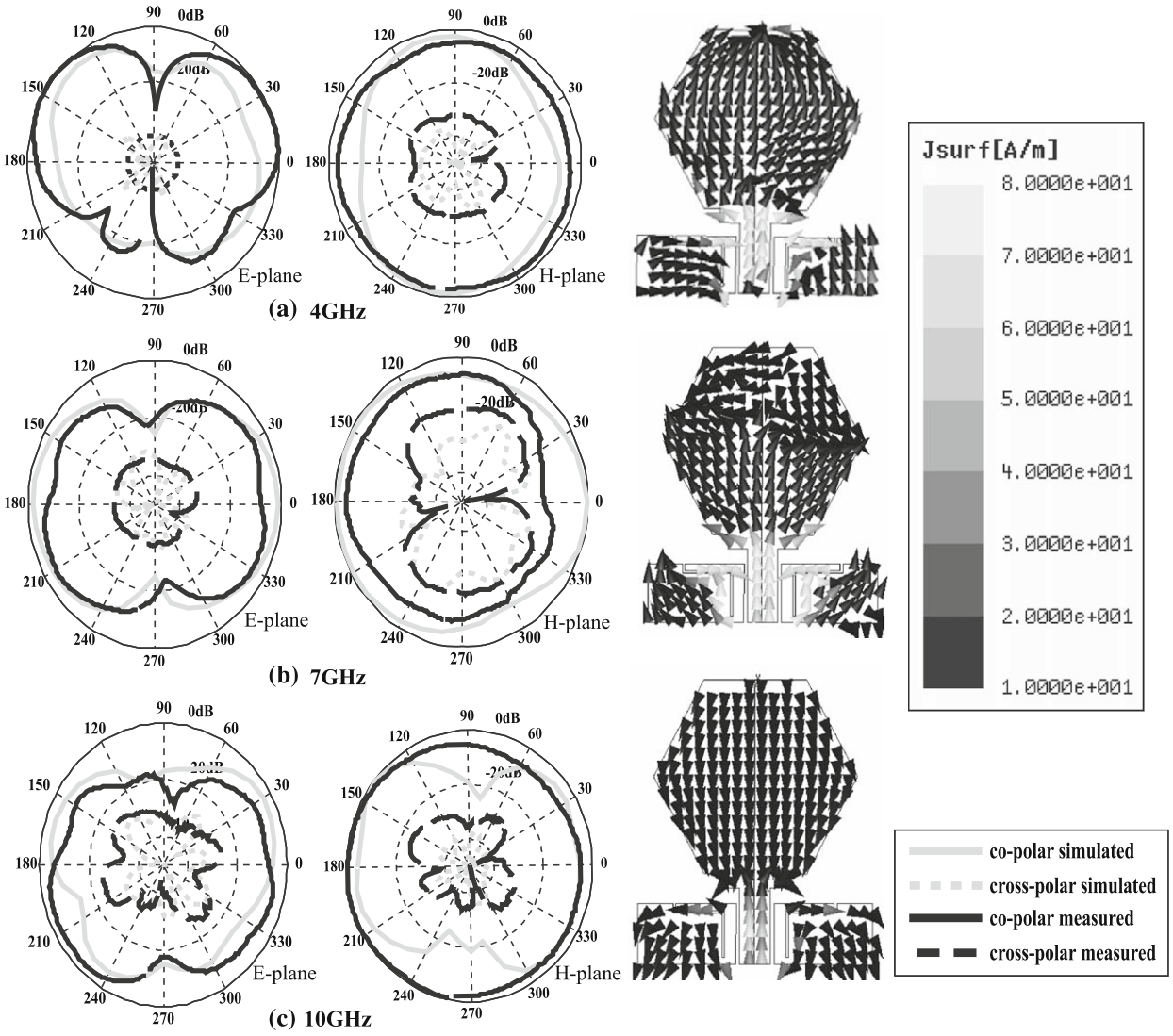

Fig. 5. Normalized simulated and measured radiation patterns and simulated current distribution of the CPW-fed monopole antenna: (a) 4 GHz, (b) 7 GHz, and (c) 10 GHz.

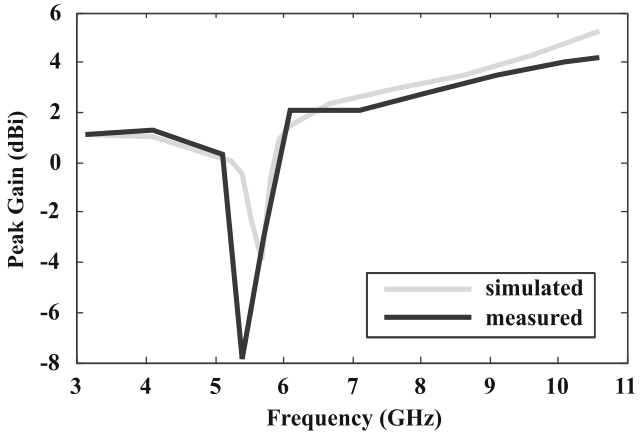

Fig. 6. The measured and simulated peak gain of the CPW fed monopole antenna.

H-plane pattern is slightly asymmetric due to the asymmetric of ACS fed antenna structure [19].

A compact (UWB+WLAN band-rejection) antenna with size of ($11.4 \times 21.5 \times 1\,mm^3$) is designed, fabricated, and tested on FR4 substrate having dielectric constant of 4.4 and thickness of 1 mm

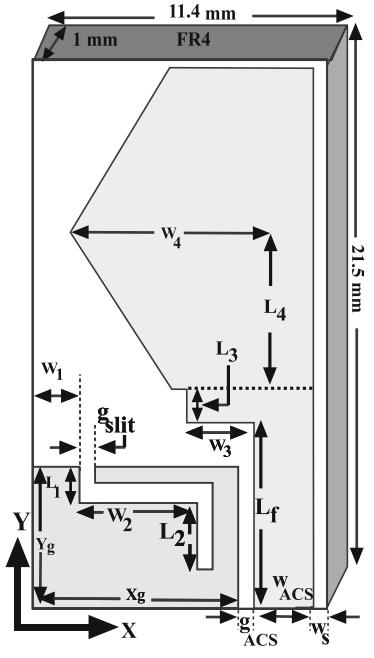

Fig. 7. Geometry of the UWB with band-notched half monopole antenna.

Please cite this article as: Soltani S, et al. Two novel very small monopole antennas having frequency band notch function using DGS for UWB application. Int J Electron Commun (AEU) (2010), doi:10.1016/j.aeue.2010.01.013

and loss tangent of (around 0.02). The half CPW-fed or asymmetric coplanar strip (ACS) fed is designed to have good matching with the signal trace width W_{ACS} (=3.2 mm) and distance between signal line and substrate edge W_s (=0.2 mm) and the signal to ground gap g_{ACS} (=0.3 mm) [16]. The ground size is $X_g \times Y_g (= 7.7\,\text{mm} \times 4.35\,\text{mm})$.

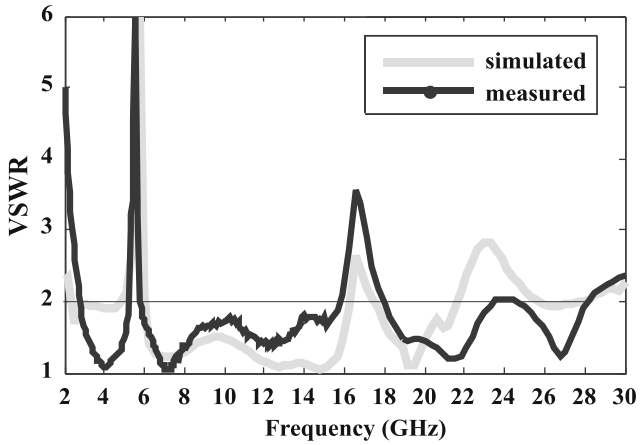

Fig. 8. Measured and simulated VSWR of the half monopole antenna.

The others final fabricated dimensions of half monopole antenna are similar to dimensions of CPW-fed monopole antenna are listed in Table 1.

4.2. Simulation and measurement results

The antenna was fed by SA6716 SMA connector. The proposed antenna was constructed and experimentally studied. Fig. 8 shows the measured and simulated frequency response of the VSWR for the proposed half monopole antenna. It is apparent that the proposed antenna can satisfy the UWB band (3–16 GHz) for $VSWR < 2$ with rejecting 5–6 GHz band. An excellent agreement can be seen between the numerical and Experimental VSWR results.

The normalized simulated and measured radiation patterns including the vertical (E_θ) and the horizontal (E_φ) polarization patterns in the elevation direction (x–z and y–z planes) and simulated current distribution at 4, 7, and 10 GHz for the proposed antenna are also studied in Figs. 9(a)–(c), respectively. Due to the asymmetry antenna structure, unsymmetrical radiation patterns are seen in the H-plane as depicted in the plots. Quasi omni-directional radiation patterns in the H-plane are observed. Fig. 9(a) shows the E fields at 4 GHz, where the electric fields are concentrated at the upper part with polarization mainly in the y-axis. This set of field distribution is locally similar to that of TE_{01} mode in a rectangular waveguide. The radiation

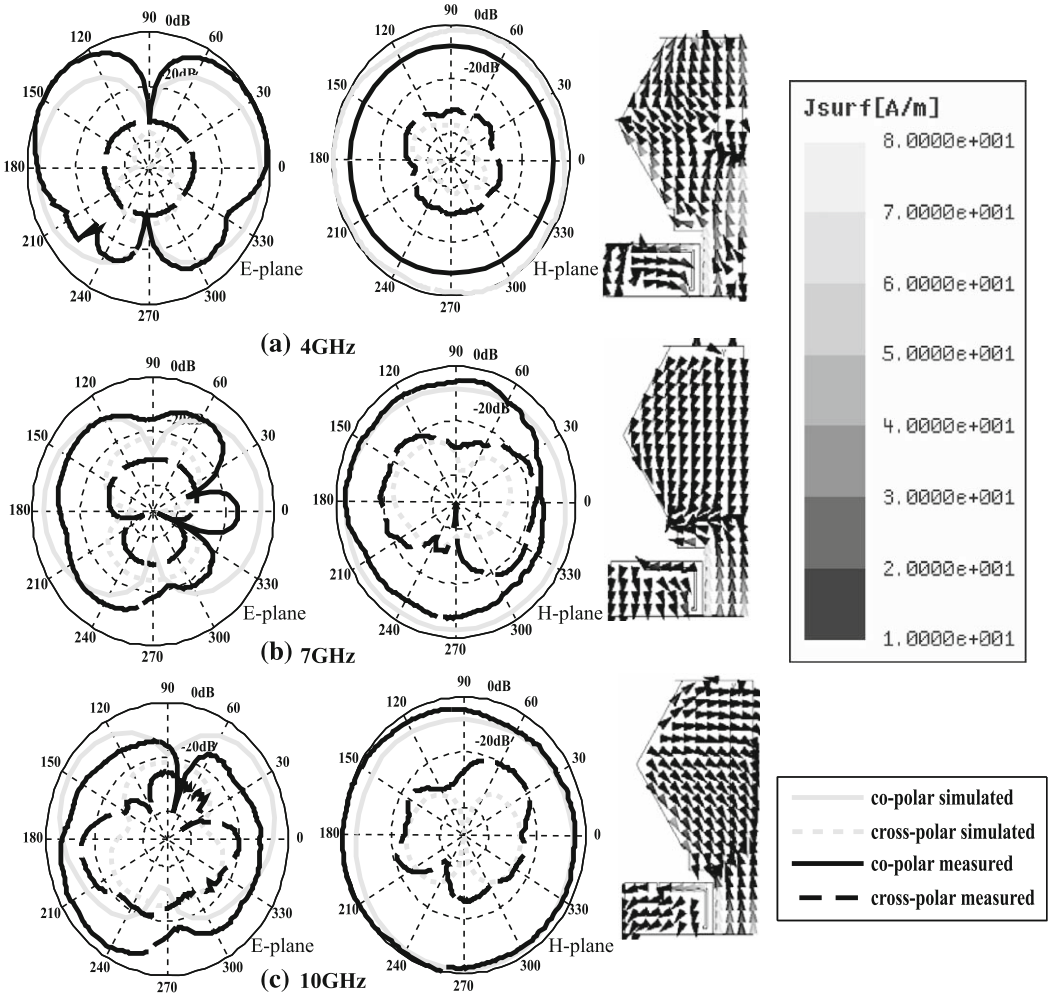

Fig. 9. Normalized simulated and measured radiation patterns and simulated current distribution of the ACS-fed half monopole antenna: (a) 4 GHz, (b) 7 GHz, and (c) 10 GHz.

Please cite this article as: Soltani S, et al. Two novel very small monopole antennas having frequency band notch function using DGS for UWB application. Int J Electron Commun (AEU) (2010), doi:10.1016/j.aeue.2010.01.013

pattern of this mode is like a small dipole oriented in the *y*-axis leading to a bidirectional pattern in the *y*–*z*-plane and omni directional pattern in the *xz*-plane, as shown in Fig. 9(a). Figs. 9(b) and (c) shows E fields at 7 and 10 GHz where both *x*- and *y*-component fields exist. Note that the *x*-component fields of the left side of the patch are unilateral. Therefore, E-plane pattern changed, as shown in Figs. 9(b) and (c). But in the symmetric structure of the CPW-fed antenna the *x*-component fields of the left and right sides of the patch are in the opposite directions that cancel out each other at far fields in the symmetric E-plane, as shown in Figs. 5(b) and (c). Therefore, the E-plane patterns are almost unchanged and still have good polarization isolation. However, the *x*-component fields generate cross-polarized patterns in the E- and H-plane, as shown in Figs. 9(b) and (c). Fig. 10 represents the simulated and measured peak gain of the antenna with the operating bandwidth. Antenna exhibits an average gain of 1.3 dBi in the operating band, except from the rejected band where it drops by approximately 5 dBi.

4.3. Comparison between performance of ACS fed and CPW fed antennas

In this part, with reference to figures presented in the previous sections, we compare measured impedance bandwidth, peak gain, radiation pattern and size of two proposed antennas. Table 3 lists this comparison data. Current distribution of two antennas at four different frequencies, 4, 5.5, 7 and 10 GHz are simulated with HFSS and displayed in Figs. 11(a)–(d), respectively. It is seen that

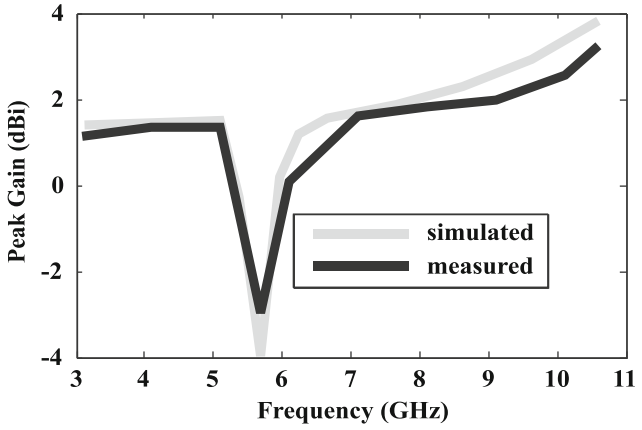

Fig. 10. The measured and simulated peak gain of the half monopole antenna.

Table 3
Comparison between performance of monopole and half monopole antennas.

Antenna characteristics	CPW-fed monopole antenna	ACS-fed half monopole antenna
BW lower UWB (GHz)	3–5	3–5
BW of WLAN rejection (GHz)	5–6	5–6
BW higher UWB (GHz)	6–15	6–15.5
E_{co} pattern in E-plane	Bi. Di.	near Bi. Di.
E_{co} pattern in H-plane	Omni. Di.	Quasi omni. Di.
Cross polar level in H-plane(dB)	Low	Low
Cross polar level in E-plane(dB)	Low	High
Peak gain (dBi) in UWB w/o filter	1.2–4.2	1.1–3.5
Min peak gain (dBi) in WLAN with filter	−8	−4
Antenna size mm^3	18.4 × 21.5 × 1	11.4 × 21.5 × 1

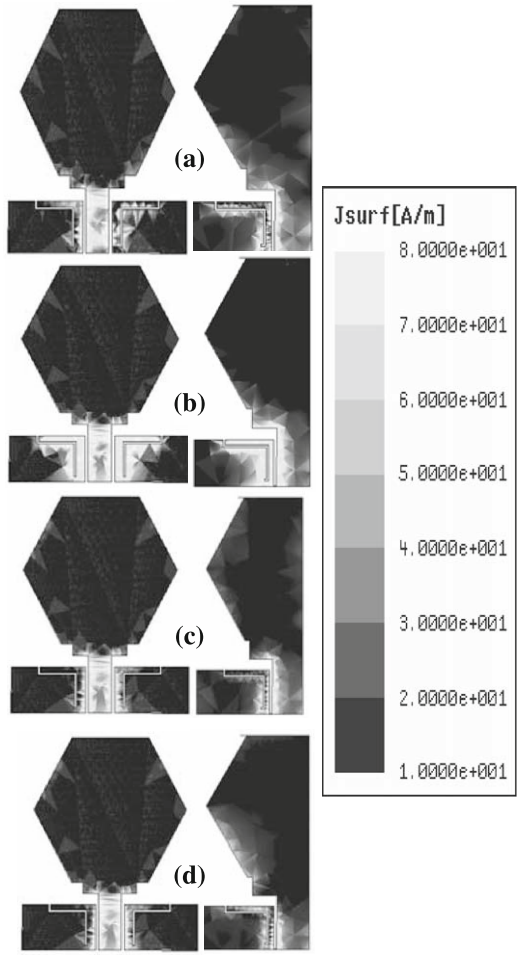

Fig. 11. Simulated results of the surface current distributions for the antenna at: (a) 4 GHz, (b) 5.5 GHz (notched band), (c) 7 GHz, and (d) 10 GHz. Right: ACS-fed half monopole antenna. Left: CPW-fed monopole antenna.

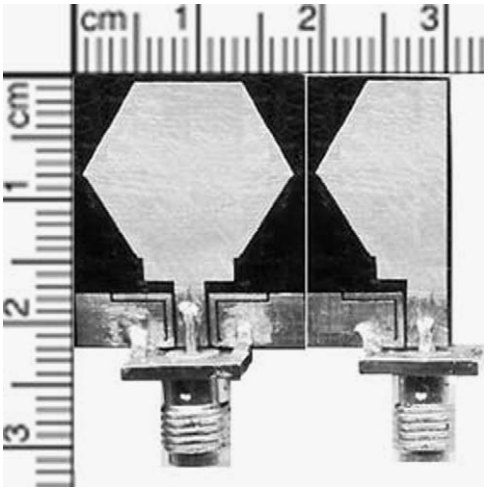

Fig. 12. Photograph of the fabricated antennas. Left: CPW-fed monopole antenna. Right: ACS-fed half monopole antenna.

the current distribution is relatively constant at 4, 7 and 10 GHz. It may be concluded that the patterns at these three frequencies will be very similar to each other. However, high density of surface current around the DGS slits was observed at 5.5 GHz, which implies that the slit resonates near 5.5 GHz. From both the measured voltage standing wave ratio (VSWR) and the simulated

Please cite this article as: Soltani S, et al. Two novel very small monopole antennas having frequency band notch function using DGS for UWB application. Int J Electron Commun (AEU) (2010), doi:10.1016/j.aeue.2010.01.013

surface current distribution, it is calculated that the DGS slits structure can help resonate at a given frequency which plays a role as a band-notched filter. The photograph of the proposed antennas printed on FR4 substrate is shown in Fig. 12. Standard photolithography was used for the fabrication.

5. Conclusion

Two very small and compact ultra wideband antennas with band-rejection characteristics are presented and discussed. A new band-rejection method using DGS is presented. Forty percent reduction in size of CPW-fed is achieved by using the ACS fed. It is realized by simply exploiting the un-miniaturized antenna structure symmetry. The effects of the various geometrical parameters on the antenna performance are studied. The uni-planar design, simple feeding technique and compactness make are easy for the integration of the antenna into circuit boards.

Acknowledgements

The authors are thankful to Urmia University and Young Researchers Club, Islamic Azad University, Urmia, Iran for financial support. The authors would also like to thank the anonymous reviewers for their thoughtful and constructive comments. The authors thank Dr. O. Azarmanesh for his professional help in editing the paper.

References

[1] New public safety applications and broadband internet access among uses envisioned by FCC Authorization of Ultra-Wideband Technology-FCC news release 2002 [Online]. Available: 〈http://www.ftp.fcc.Gov/Bureaus/Engineering_Technology/News_Releases/2002/nret0203.pdf〉.
[2] IEEE 802.15.3a Task Group. [Online] Available: 〈http://www.ieee802.org/15/pub/TG3a.html〉.
[3] Verbiest J, Vandenbosch G. A novel small-size printed tapered monopole antenna for UWB WBAN. IEEE Antenna Wireless Propag Lett 2006;5:377–9.
[4] Liang J, Chiau C, Chen X, Parini C. Study of a printed circular disc monopole antenna for UWB systems. IEEE Trans Antennas Propag 2005;53:3500–4.
[5] Jilkova J, Radia Z. Ultra-wideband coplanar-fed monopoles: a comparative study. Radio Eng 2007;17:37–40.
[6] Kim J, Yoon T, Kim J, Choi J. Design of an ultra wide-band printed monopole antenna using FDTD and genetic algorithm. IEEE Microw Wireless Compon Lett 2005;15:395–7.
[7] Cho Y, Kim K, Choi D, Lee S, Park S. A miniature UWB planar monopole antenna with 5-GHz band-rejection filter and the time-domain characteristics. IEEE Trans Antennas Propag 2006;54:1453–60.
[8] Lee Y, Sun J, Choi D, Ma T, Li C. A tapered monopole antenna with band notch function for ultra- wideband. Presented at the international conference, August 2007.
[9] Chung K, Kim J, Choi J. Wideband microstrip-fed monopole antenna having frequency band-notch function. IEEE Trans Antennas Propag 2005;15:766–8.
[10] Nikolaou1 S, Kim B, Kim K, Papapolymerou J, Tentzeris M. CPW-fed ultra wideband (UWB) monopoles with band rejection characteristic on ultra thin organic substrate. Presented at the Micro. conference, Asia-Pacific, December 2006. p. 2010–3.
[11] Gao Y, Ooi B, Popov A. Band-notched ultra-wideband ring monopole antenna. Microw Opt Technol Lett 2006;48:125–6.
[12] Kim K, Cho Y, Hwang S, Park S. Band-notched UWB planar monopole antenna with two parasitic patches. Electron Lett 2005;41:783–5.
[13] Tzyh M, Sung W. Ultrawideband band-notched folded strip monopole antenna. IEEE Trans Antennas Propag 2007;55:2473–9.
[14] Chen S, Mulgrew B, Grant P. A miniature a planar monopole antenna design with band-notched characteristics. IEEE Trans Antennas Propag 2007;55:288–92.
[15] Ansoft high frequency structure simulation (hfss), version 10. Ansoft Corporation; 2005.
[16] Garg P, Bhartia P, Bahl I. Microstrip antenna design hand book, 1st ed. House; 2001. p. 794–5.
[17] Lim J, Kim C, Lee Y, Ahn D, Nam S. A spiral-shaped defected ground structure for coplanar waveguide. IEEE Microw Wireless Compon 2002;12:330–2.
[18] Liu W. Design of a multiband CPW-fed monopole antenna using a particle swarm optimization approach. IEEE Trans Antennas Propag 2005;53:3273–9.
[19] Deepu V, Rohith K, Manoj J, Suma M, Mohanan P. Compact asymmetric coplanar strip fed monopole antenna for multiband applications. IEEE Trans Antennas Propag 2007;55:377–9.
[20] Sun M, Zhang Y. Miniaturization of planar monopole antennas for ultrawideband applications. In: Proceedings of the antenna technology and small and smart antennas metamaterials, Cambridge, 2007. p. 197–200.
[21] Sun M, Zhang Y. Ltcc-based compact UWB antenna ant its integration study. Micro Opt Technol Lett 2008;50:789–93.
[22] Wang X, Chen X, Guo L, Parini C. Towards miniaturization of UWB antennas. UWB 2007 European workshop, Grenoble, France, May 2007. p. 3500–4.

Saber Soltani was born in Urmia, Iran, in March 1983. He received the B.S. degree in Electrical and Telecommunication Engineering from the Urmia Azad University, in 2006 and M.Sc. degree in Electrical and Telecommunication Engineering from Urmia University, Urmia, Iran, in 2008. He is currently working toward Ph.D. degrees in Microelectronics Research Laboratory, Urmia University, Urmia, Iran. He is a member of Iranian Society of Electrical Engineers and young researcher club of Urmia Azad University. He is the author or coauthor of several refereed journal articles and conference papers. His research interests include antenna miniaturization, optimization method, monopole antennas, slot antennas, hybrid antennas, circular polarization antennas, diversity antennas, mobile phone and wireless local-area network antennas, and their antenna applications.

Mohammad Naghi Azarmanesh was born in Tabriz, Iran, in 1950. He received the B.S. degree in Physics from Tabriz University, Iran, in 1973, the M.S. degree in Electrical Engineering from the University of Paris VI in 1976, and Ph.D. degree in Electrical Engineering from Polytechnique De Toulouse, France. In 1979 he joined Applied Physics Department in Urmia University, where he worked effectively in founding Electrical Engineering Department in 1983. In 1998 he worked with three other colleagues in developing Microelectronics Research Center in Urmia University. He is currently the head of Microelectronics Research Center. Dr. Azarmanesh is a member of Iranian Society of Electrical Engineers and member of IEEE, Institute of Electronics, Information and Communication Engineers (IEICE) of Japan. He has published a book, Elecrtomagnetic Field Theory (Urmia: Urmia University, 1996).

Parisa Lotfi was born in Urmia, Iran, in May 1984. She received the B.S. degree in Electrical Engineering from the Urmia Azad University, in 2008. She is currently working toward the B.S. degree in Mathematics and M.S. degree in Electrical Engineering in Urmia University. She is a member of Iranian Society of Electrical Engineers Her current research interests are in antenna design, numerical methods in electromagnetic.

Gholamreza Dadashzadeh was born in Urmia, IRAN, in 1964. He received the B.Sc. degree in communication engineering from Shiraz University, Shiraz, Iran in 1992 and M.Sc. and Ph.D. degree in Communication Engineering from Tarbiat Modarres University (TMU), Tehran, Iran, in 1996 and 2002, respectively. From 1998 to 2003, he has worked as head researcher of Smart Antenna for Mobile Communication Systems (SAMCS) and WLAN 802.11 project in Radio Communications group of Iran Telecomm Research Center (ITRC). From 2004 to 2008, he was dean of Communications Technology Institute (CTI) in ITRC. He is currently as Assistance Professor in the Department of Electrical Engineering at Shahed University, Tehran, Iran. Dr. Dadashzadeh is a member of IEEE, Institute of Electronics, Information and Communication Engineers (IEICE) of Japan and Iranian Association of Electrical and Electronics Engineers (IAEEE) of Iran.

Please cite this article as: Soltani S, et al. Two novel very small monopole antennas having frequency band notch function using DGS for UWB application. Int J Electron Commun (AEU) (2010), doi:10.1016/j.aeue.2010.01.013